

CHAPTER 2 THEORY AND REVIEW

The objective of this current research was to synthesize and characterize copper(II) mixed carboxylates as thermally-stable, low-temperature, magnetic and redox-active metallomesogens. Thus, this chapter focuses on the chemistry of copper(II) carboxylates, metallomesomorphism, and the instrumental techniques used to characterize the metallomesogens, specifically CHN elemental analyses, FTIR spectroscopy, molar conductivity, UV-vis spectroscopy, thermogravimetry (TGA), differential scanning calorimetry (DSC), optical polarized microscopy (OPM), magnetic susceptibility, and cyclic voltammetry (CV).

2.1 COPPER(II) CARBOXYLATES – AN INTRODUCTION

Copper is a first-row transition metal with valence electronic configuration $4s^1 3d^{10}$. As such, it can be quite easily oxidized to Cu(I) ($3d^{10}$), which in turn undergoes an easier oxidation to Cu(II) ($3d^9$). However, further oxidation to Cu(III) ($3d^8$) is difficult. Thus, it forms mainly Cu(I) (less stable) and Cu(II) (more stable) compounds.

The Cu(II) ion forms labile coordination complexes, and has shown special preference for N-donor ligands, such as NH_3 (ammonia), $\text{C}_5\text{H}_5\text{N}$ (pyridine), and 2,2'-bipyridine. The metal ion is also geometrically flexible as it can easily adapt to changing number of ligands. Thus, complexes with octahedral, square pyramidal, trigonal bipyramidal, square planar, and tetrahedral geometries have been reported. Also, because of the d^9 configuration, ligands in an octahedral

environment are subjected to strong Jahn-Teller distortion, resulting (in most cases) in an elongated octahedron or a square planar geometry.

Copper(II) carboxylates are normally dinuclear complexes with the general formula $[\text{Cu}_2(\text{RCOO})_4]$, where R may be an alkyl or aryl group. The carboxylate ion may bind to Cu(II) in a variety of modes, such as monodentate, bidentate, bridging, and chelating. These complexes may be prepared by several methods, such as metathesis [1-7], ligand-exchange [8], and one-pot reaction [9]. A few examples are discussed below.

A mononuclear $[\text{Cu}(\text{CH}_3\text{COO})_2(\text{bpy})]$, reported by Koo [10], was obtained by adding 2,2'-bipyridine to $[\text{Cu}(\text{CH}_3\text{COO})_2]\cdot\text{H}_2\text{O}$ in dimethylformamide (DMF). The crystal structure reveals that the complex was square planar with CH_3COO^- and 2,2'-bipyridine as monodentate and chelating bidentate ligand, respectively (**Figure 2.1**).

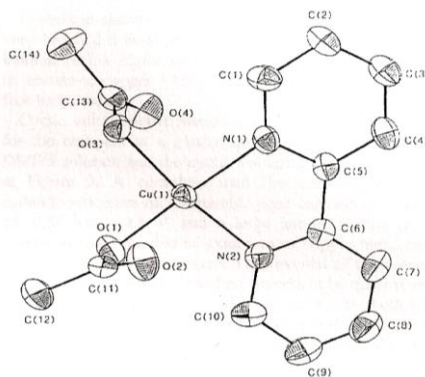


Figure 2.1 Crystal structure of $[\text{Cu}(\text{CH}_3\text{COO})_2(\text{bpy})]$

Another mononuclear complex is $(\text{NH}_4)_2[\text{Cu}(\text{DIMMAL})_2]\cdot 4\text{H}_2\text{O}$, where DIMMAL is 2-di-1H-2-imidazolylmethylmalonate. It was obtained as a rectangular purple crystal by Nunez *et al.* [11] by mixing $\text{Na}_2(\text{DIMMAL})\cdot 5\text{H}_2\text{O}$

with copper(II) chloride, and then adding solid ammonium chloride to the purple–blue solution formed. The crystal structure shows that the DIMMAL ligands were centrosymmetrically arranged around Cu(II) ion through two imidazole nitrogen atoms and one carboxylate oxygen atom. Therefore, the Cu(II) ion adopted a tetragonally elongated octahedral geometry. The basal octahedron plane was made up of four nitrogen atoms from four imidazole rings (**Figure 2.2**).

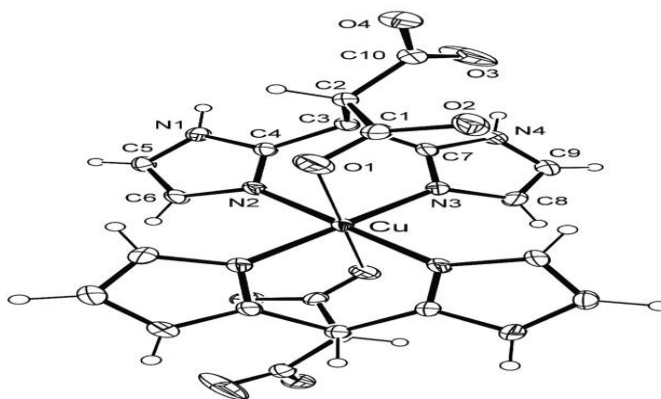


Figure 2.2 Crystal structure of $(\text{NH}_4)_2[\text{Cu}(\text{DIMMAL})_2] \cdot 4\text{H}_2\text{O}$

Yenikaya *et al.* [12] reported a binuclear mixed-ligand copper(II) complex, $\text{di-}\mu\text{-(2-aminopyridine-N,N')bis(2,6-pyridinedicarboxylate)aqua}$ copper(II) tetrahydrate, formulated as $[\text{Cu}(\mu\text{-ap})(\text{dipic})(\text{H}_2\text{O})]_2 \cdot 4\text{H}_2\text{O}$, where dipic is 2,6-pyridinedicarboxylate, and ap is 2-aminopyridine. The complex formed green crystals, and its crystal structure shows the central Cu(II) ion residing on a centre of symmetry in a distorted square-pyramidal coordination environment comprising of two N atoms (one from dipic and one from the ap ring), two carboxylate O atoms from dipic, and one O atom from water (**Figure 2.3**). It was

suggested that intermolecular N–H---O and O–H---O hydrogen bonds and π - π stacking interactions were effective in stabilizing the crystal structure.

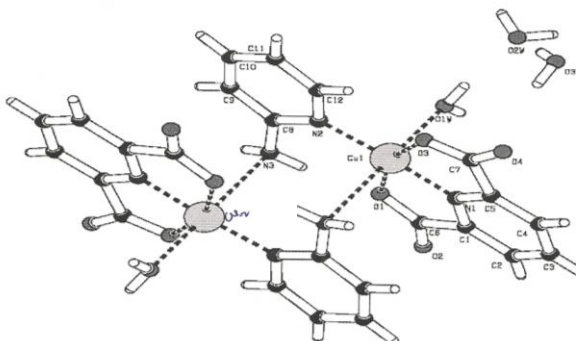


Figure 2.3 Crystal structure of $[\text{Cu}(\mu\text{-ap})(\text{dipic})(\text{H}_2\text{O})]_2 \cdot 4\text{H}_2\text{O}$

Melnik *et al.* [13] reported a dinuclear bis(μ -benzoato-O,O')(dimethylsulphoxide)copper(II), $[\text{Cu}(\text{C}_6\text{H}_5\text{COO})_2(\text{DMSO})_2]_2$, obtained as dark green crystals when anhydrous copper(II) benzoate was dissolved in DMSO. The complex has a dimeric and square pyramidal geometry at each Cu(II) centre bridged by four benzoato ligands at the equatorial positions and DMSO at the axial positions (**Figure 2.4**).

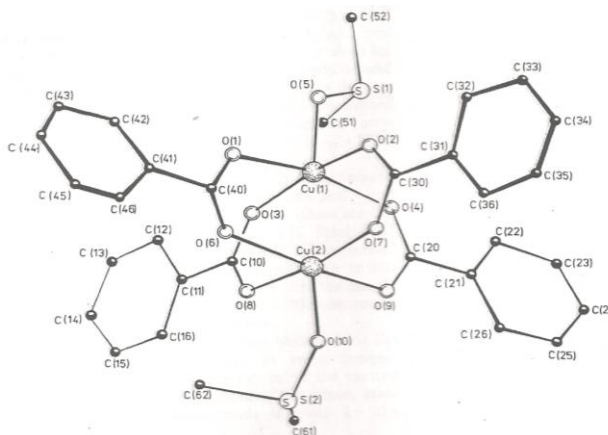


Figure 2.4 Crystal structure of $[\text{Cu}(\text{C}_6\text{H}_5\text{COO})_2(\text{DMSO})]_2$

Youngme *et al.* [14] reported two dinuclear tetracarboxylato-bridged Cu(II) complexes, $[\text{Cu}_2(\mu\text{-O}_2\text{CC}_6\text{H}_4\text{OH})_4(\text{C}_7\text{H}_7(\text{NO})_2)] \cdot 6\text{H}_2\text{O}$ (**Figure 2.5**) and $[\text{Cu}_2(\mu\text{-O}_2\text{CCH}_3)_4(\text{C}_7\text{H}_7\text{NO})_2]$ (**Figure 2.6**), where $\text{O}_2\text{CC}_6\text{H}_4\text{OH}$ is 3-hydroxybenzoate and $\text{C}_7\text{H}_7\text{NO}$ is 4-acetylpyridine. The complexes were made up of dinuclear units, in which two Cu(II) ions were bridged by four *syn,syn*- $\eta^1:\eta^1:\mu$ carboxylates, showing a paddle-wheel cage type with a square-pyramidal geometry, arranged in different ways.

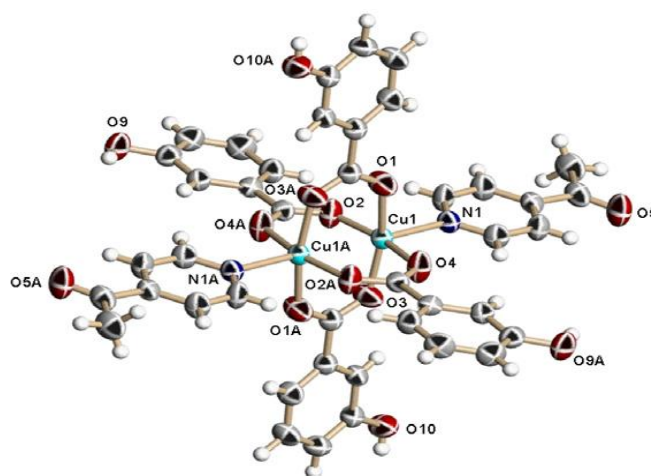


Figure 2.5 Crystal structure of $[\text{Cu}_2(\mu\text{-O}_2\text{CC}_6\text{H}_4\text{OH})_4(\text{C}_7\text{H}_7(\text{NO})_2)] \cdot 6\text{H}_2\text{O}$

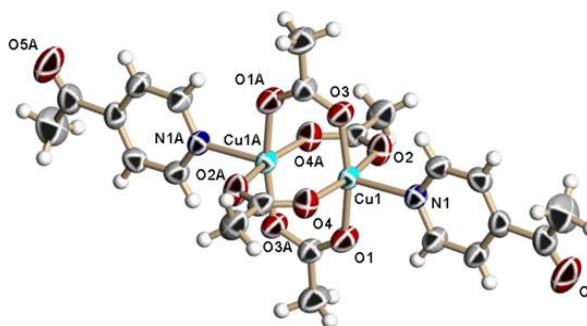


Figure 2.6 Crystal structure of $[\text{Cu}_2(\mu\text{-O}_2\text{CCH}_3)_4(\text{C}_7\text{H}_7\text{NO})_2]$

Perlepes *et al.* [6] reported that treating $[\text{Cu}_2(\text{CH}_3\text{COO})_4(\text{H}_2\text{O})_2]$ with two equivalent of 2,2'-bipyridine (bpy) in MeCN yielded $[\text{Cu}_2(\text{CH}_3\text{COO})_4(\text{bpy})_2]\cdot\text{H}_2\text{O}$ involving two *syn-anti* acetate bridges in the form of infinite ladder-like chains as a result of hydrogen-binding interactions with the water molecules (**Figure 2.7**)

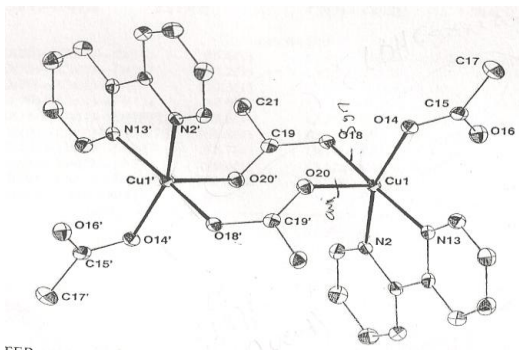


Figure 2.7 Crystal structure of $[\text{Cu}_2(\text{CH}_3\text{COO})_4(\text{bpy})_2]\cdot\text{H}_2\text{O}$

Hadadzadeh *et al.* [15] obtained an ionic binuclear Cu(II) complex, $[\{\text{Cu}(\text{phen})_2\}_2(\mu\text{-CH}_3\text{COO})](\text{PF}_6)_3$, where phen is 1,10-phenanthroline, by dissolving $[\text{Cu}_2(\text{CH}_3\text{COO})_4]\cdot 2\text{H}_2\text{O}$ and 1,10-phenanthroline in methanol followed by addition of an excess NH_4PF_6 . The crystal structure shows two independent Cu(II) ions, with different geometry around each copper center, and were bridged by an acetate anion. The acetate-bridged ligand shows a *syn-anti* coordination mode with a trigonal bipyramidal geometry for one of the Cu(II) center and a distorted square-based pyramidal geometry for the other Cu(II) center (**Figure 2.8**).

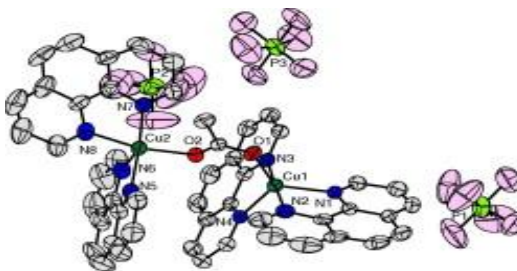


Figure 2.8 Crystal structure of $[\{Cu(phen)_2\}_2(\mu-CH_3COO)][PF_6]_3$

Baran *et al.* [8] reported a distorted square pyramidal binuclear $[Cu(sup)_2CH_3CN]_2$ ($sup = \alpha$ -methyl-4-(2-thienyl-carbonyl)phenylacetic acid), obtained from the ligand-exchange reaction between $[Cu(sup)_2H_2O]_2$ and acetonitrile. The crystal structure shows *syn-syn* coordination mode with a distorted square pyramidal Cu(II) centres (**Figure 2.9**).

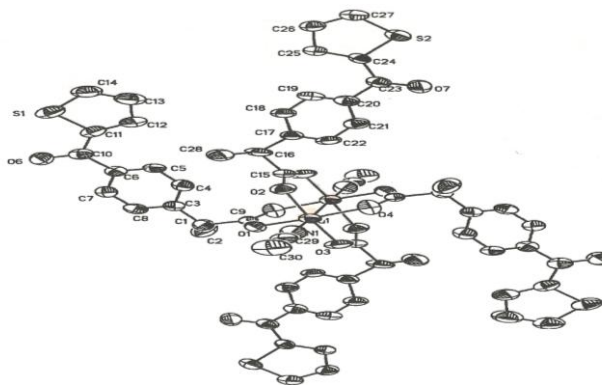


Figure 2.9 Crystal structure of $[Cu(sup)_2CH_3CN]_2$

Inoue *et al.* [16] synthesized polymeric copper(II) benzoate trihydrate from aqueous solution of copper(II) sulphate and sodium benzoate by diffusion

method. The crystal structure shows Cu(II) atoms linked by water molecules and the benzoate group (**Figure 2.10**).

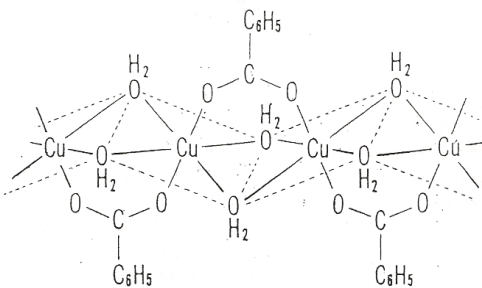


Figure 2.10 *Crystal structure of polymeric copper(II) benzoate trihydrate*

2.2 SELECTED PROPERTIES OF COPPER(II) CARBOXYLATES

2.2.1 *Thermal properties*

Thermal analysis is becoming an essential tool for material research. This is reflected in the frequency of thermo-analytical investigations during the period of 1975-1987 of about 15-20% in the *Journal of Thermal Analysis*. The compounds studied were mostly inorganic and coordination compounds [17]. Two common thermal methods are thermogravimetry (TGA) and differential scanning calorimetry (DSC).

TGA measures the mass (weight) of a sample in a specified atmosphere as the temperature of the sample is programmed. The most common temperature program is a linear increase in temperature with time, although isothermal programs, stepped temperature programs, and so on may also be used. In the most common of TGA experiments, the sample temperature is increased linearly over a time period and the mass of the sample is constantly recorded. The output from a TGA experiment is a plot of weight (or weight %) vs. temperature.

Weight or weight % is plotted along the y -axis and temperature (or time for a linear temperature ramp) along the x -axis. The change in weight of a sample as the temperature changes provides several informations. First, this determines the temperature at which the material loses (or gains) weight. Loss of weight indicates evaporation and/or decomposition. A gain in weight can indicate adsorption by the sample of a component in the atmosphere or a chemical reaction with the atmosphere. Second, the temperatures at which no weight change takes place indicate the temperature stability of the material. These weight changes at certain temperatures are physical properties of chemical compounds under the conditions of the experiment (atmosphere, heating rate). This information can be used to determine if a sample is the same as a “standard” or “good” material in a production process [54].

While performing TGA, the weight of the sample is measured as a function of sample temperature or time [55]. Thermogram or thermal curve is a plot of the mass or the percentage of the initial mass as the function of temperature or time. The curve produced in TGA experiment is due to the weight changes when decomposition of the samples takes place in one or several different ways or by reaction with the surrounding atmosphere.

The sample is placed in the sample pan constructed of platinum, aluminium or alumina. Most studies used weight of between 5 and 25 mg. The sample is then enclosed in the electric furnace typically cover the temperature from the ambient temperature up to 1000°C. Most studies also use systems that continuously purged the furnace and the sample with a gas. The common gases

used for purging are nitrogen or argon if an inert atmosphere is required, or oxygen if an oxidative atmosphere is needed. The temperature of the furnace is monitored by using a thermocouple that is placed near the sample but not in contact with it to avoid creating an error in the temperature of the thermal curve. The temperature differential between the thermocouple and the sample depends on the gas flow rate, the heating rate, and the thermal conductivity of the gaseous environment in the furnace. Modern TGA instruments use computers to provide a controlled system over the operational parameters. The heating rate can be programmed and adjustable between 0.1 to 200°C/min. Thermal equilibrium is normally established in 30 s.

In order to perform the measurement, some considerations should be taken into account. The first and foremost is the sample preparation. The weight of the sample should be adequate for the test and the sample should not be contaminated with the sample preparation process. Furthermore, the morphology of the sample also needs to be considered. The reaction is faster in the powdered sample rather than a coarse sample because the gaseous reaction products can reach the surface of the individual powder grain more quickly.

TGA cannot be used to study processes that do not involve weight changes, such as melting points. The change in weight is very important for quantitative analysis, while the temperature at which the changes take place is useful for qualitative analysis.

DSC is an instrumental technique to measure the heat capacity or heat changes at isobaric conditions [46]. An example of a DSC trace is shown in **Figure 2.11**.

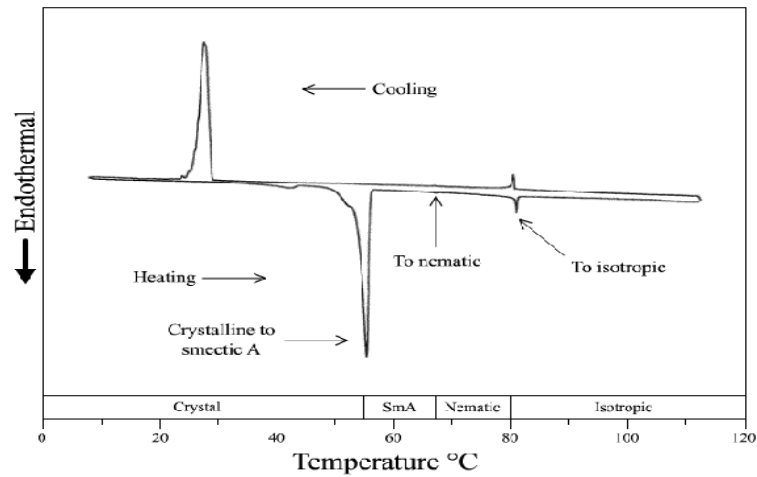


Figure 2.11 An example of a DSC trace

Physical properties that related to the heat changes, such as melting, crystallization and vaporization, can be monitored by using DSC. Generally, DSC was used to determine glass transition temperature (T_g), melting temperature (T_m), specific heat (ΔC_p) as well as heat of fusion (ΔH_{fus}).

DSC instrument can analyzed liquid or solid samples (film, powder, crystal or granule). The solid sample should be encapsulated in an aluminium pan to prevent contamination and in good thermal contact with the furnace. For liquid sample, a type of pan that can withstand any internal pressure may be used. Consideration should be given when choosing the pans and encapsulating the samples to avoid wrong data collection [55].

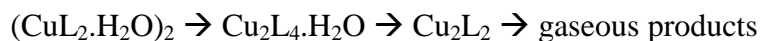
The most common scan rate used is 10°C/min. Choice of scan rate can affect the sensitivity, temperature calibration, resolution, transition kinetic, and time of analysis [55].

The normal weight of a sample may vary between 0.5 mg and 1.0 mg. Small samples permit higher scan rate, yield maximum resolution and thus better qualitative results, and are recommended where the transition energy to be measured is very high. On the other hand, large samples permit observation of small transition and yield more precise quantitative measurements.

The thermal behavior of several hydrated copper(II) carboxylates complexes was studied by Micera *et al.* [18]. The authors found that the dehydration temperature of coordinated water molecules was higher (143°C) for a mononuclear $[\text{Cu}(\text{2,6-dihydroxybenzoate})_2(\text{H}_2\text{O})_2]$, indicating that the water molecules were strongly held by the metal due to the shorter Cu-O(water) bond distance or by the involvement of water in strong intramolecular (to the carboxylic group) and intermolecular (to the phenolic group) bonds. In contrast, the water molecules were released at a lower temperature (< 100°C) from $[\text{Cu}(\text{N-acetylglycinate})_2(\text{H}_2\text{O})_2] \cdot 2\text{H}_2\text{O}$ and $[\text{Cu}_2(\text{salicylate})_2(\text{H}_2\text{O})_2] \cdot 2\text{H}_2\text{O}$, indicating the coordinated and uncoordinated water molecules were hydrogen-bonded to each other.

W.Brzyka *et al.* [19] synthesized and studied the thermal decomposition of Cu(II) complex with 2,6-dichlorobenzoic acid in air atmosphere. They found that on heating, the hydrated complex $[\text{Cu}(\text{C}_7\text{H}_3\text{O}_2\text{Cl}_2)_2 \cdot \text{H}_2\text{O}]_2$ lost the molecules of water of crystallization in two steps at 122°C and 147°C. The authors suggested

that the higher dehydration temperature of this complex was because the water molecules were strongly bonded to Cu(II). It was noticed that on heating, the complex decomposed to gaseous products, probably a chloroorganic compounds of copper without forming a solid residue. The decomposition process of Cu(II) complex of 2,6-dichlorobenzoate (L) is summarized below.



2.2.2 Metallomesogens

Metallomesogens are metal-based liquid crystals [20-23]. The presence of metal ions, such as first-row transition metals, results in materials having the combined advantage of anisotropy and fluidity of liquid crystals with useful properties associated with the presence of polarizable *d* electrons, such as tunable geometry and colour, thermal stability, electronic conductivity, and magnetic and redox properties.

Liquid crystal (LC) is a state of matter that has properties of both solid and liquid. LC behaves like crystal in term of the arrangement of its molecules, and it is fluid like a liquid (**Figure 2.12**).

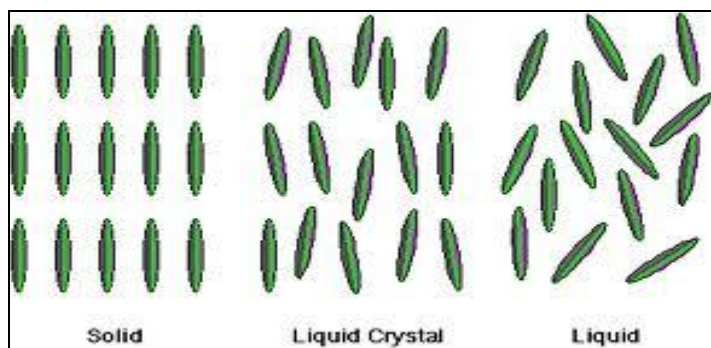


Figure 2.12 *The different arrangement of particles in solid, liquid crystal, and liquid states*

There are several terms specifically used in LC; some of these terms and their description are listed in **Table 2.1**.

Table 2.1 *Liquid crystal terms*

Term	Description
Mesophase	Liquid crystal phases that can be characterized by the type of ordering or symmetry.
Mesogenic	Something which is ‘liquid-crystal like’ but does not necessarily has liquid crystal properties. Part of liquid crystal molecules responsible for mesophase formation.
Mesomorphic	Something that shows the liquid crystal behavior.
Metallomesogen	Metal-containing liquid crystal. Mesogen that contain metal atom.
Anisotropic	The property of being directionally dependent.
Isotropic	Identical properties in all directions.
Birefringence	The splitting of a ray of light into two when it passes through certain anisotropic materials, such as crystals of calcite or boron nitride.

The idea of the development of LC is to destroy the order of the solid state through two possibilities, namely by the effect of solvent (lyotropic LC) or the action of temperature (thermotropic LC).

Optical polarized microscope is used to observe and photograph specimens that are visible primarily due to their optically anisotropic character. Anisotropic substances, such as uniaxial or biaxial crystals, oriented polymers, or liquid crystals, generate interference effects in the polarized light microscope, which result in differences of color and intensity in the image as seen through the eyepieces and captured on film, or as a digital image.

This technique is useful for orientation studies of doubly refracting media that are aligned in a crystalline lattice or oriented through long-chain molecular interactions in natural and synthetic polymers and related materials. Also investigated in polarized light are stresses in transparent singly refracting media (for example, glass) and the identification and characterization of a wide spectrum of anisotropic substances through their refractive index and birefringence.

Currently, LCs are classed according to their shape and their mesophase, such as nematic, smectic, chiral nematic (cholesteric), calamitic and discotic [24]. Specific examples are discussed below.

Attard *et al.* [1] reported that copper(II) carboxylates can promote the formation of discotic mesophase [Figure 2.13]. This behavior is a consequence of the disc-like shapes of the polar cores of the molecules which consist of two copper(II) ions coordinated with four carboxylate groups. These dinuclear carboxylates have low magnetic moments due to the spin exchange between the unpaired electrons in each copper ion. It was suggested that the combination of discotic mesophase and the electronic properties of the dinuclear cores could lead to interesting conductance effect [25].



Figure 2.13 *Discotic mesophase*

The discotic mesophase of copper(II) complexes of straight chain aliphatic carboxylates, studied by X-ray diffraction, showed columnar stacks of the dimers with the columns arranged on a hexagonal lattice [25-27]. The transition temperature between the crystalline phase and the columnar hexagonal mesophase ranges from 85°C to 120°C.

The crankshaft appearance of the columnar, studied by Extended X-Ray Absorption Fine Structure (EXAFS), reveals weak bonds between the oxygen atoms of the carboxylate groups of one dimer and the free octahedral sites on the copper ions in the neighboring dimer. These bonds are believed to further stabilize the complex [28].

It has been reported that unsymmetrical compounds have lower melting points than symmetrical compounds, and that the clearing point increases when the chain length increase [29]. For example, $[\text{Cu}_2(\text{CH}_3(\text{CH}_2)_{14}\text{COO})_4]$ has a melting temperature of 112°C and clearing temperature of 220°C, whereas $[\text{Cu}_2((\text{CH}_2)_7)_2\text{CHCOO})_4]$ has the melting temperature of -20°C and clearing temperature of 214°C [1]. Linear chains also enhance the anisotropy of the system and the fact that they are flexible and do not crystallize easily lead to lowering of their melting temperature.

Rao *et al.* [30] reported a mesogenic (nematic) Schiff-base of N,N'-di-4-(4'-pentyloxybenzoate)salicylidenediaminoethane, H_2dpbsde (abbreviated as H_2L^5) (**Figure 2.14**). The authors studied the mesogenic properties of H_2L^5 as well as $[\text{NiL}^5]_2$ and $[\text{CuL}^5]$ complexes (**Figure 2.15**), using polarized optical microscopy and differential scanning calorimetry (DSC).

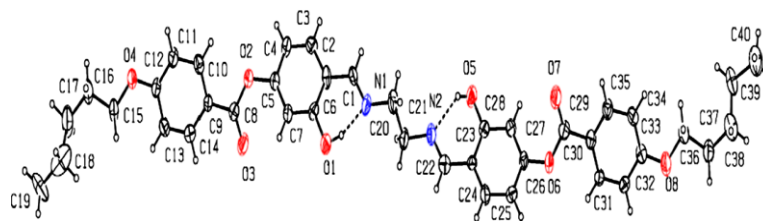


Figure 2.14 Crystal structure of H_2L^5

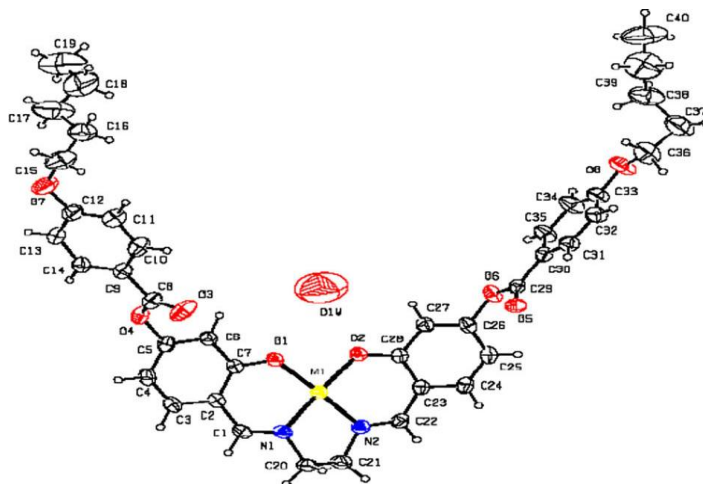


Figure 2.15 Crystal structure of $[ML^5]$ [$M = Ni$ or Cu]

The introduction of the metal ion into the metal-coordination sphere, as expected, resulted in the elevation of the transition temperature, melting and clearing points. The assignment of the mesophase (nematic) in each case was on the basis of the optical textures (**Figure 2.16**) and the DSC thermograms. From DSC, the transition temperatures for the ligand (H_2L^1) were: crystal to nematic (crys-N), 175°C; nematic to isotropic liquid (N-I), 229°C; and isotropic liquid to nematic (I-N), 216°C. For $[NiL^5]_2$, the transition temperatures were crys-crys, 145°C; crys-N, 245°C; and N-I (decompose), 255°C; whereas for $[CuL^5]$, crys-crys, 136°C; crys-N, 225°C; N-I, 261°C; and N-crys, 200°C.

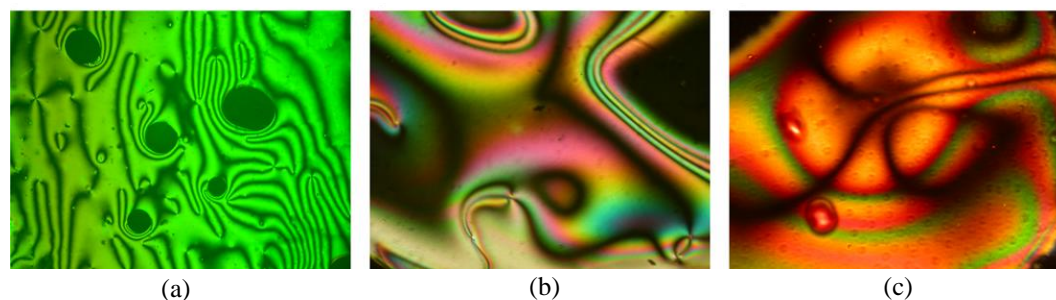


Figure 2.16 Optical textures of: (a) H_2L^5 at $210^\circ C$, (b) $[NiL^5]$ at $252^\circ C$, and (c) $[CuL^5]$ at $245^\circ C$

Rao *et al.* [31] reported a mesogenic property of Schiff base, N,N'-di-(4-hexadecyloxysalicylidene)diaminoethane, $H_2dhdsde$ (abbreviated as H_2L^1) (**Figure 2.17**) that exhibit smectic-C (SmC) mesophase.

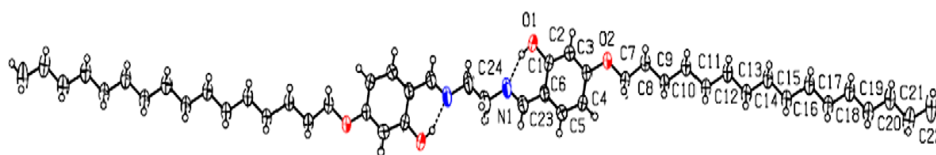


Figure 2.17 Crystal structure of H_2L^1

Complex of H_2L^1 with La^{III} shows smectic-X (SmX) mesophase, while that of Pr^{III} shows smectic-F (SmF) and smectic-C (SmC) mesophases. From the DSC, the transition temperatures for the ligand were: crys-crys, $76^\circ C$; crys-SmC, $94^\circ C$; SmC-I, $102^\circ C$; I-SmC, $101^\circ C$; crys-crys, $71^\circ C$. For $[La(L^1H_2)_3NO_3](NO_3)_2$, the transition temperatures were: cryst-crys, $90^\circ C$; crys-SmX, $93^\circ C$; SmX-I(decompose), $200^\circ C$. For $[Pr(L^1H_2)_3NO_3](NO_3)_2$, the transition temperatures were: crys-SmF, $113^\circ C$; SmF-SmC, $173^\circ C$; SmC-I (decompose), $240^\circ C$. The

optical texture of the ligand, La^{III} and Pr^{III} as well as the crystal structure of the ligand, are shown in **Figure 2.18**.

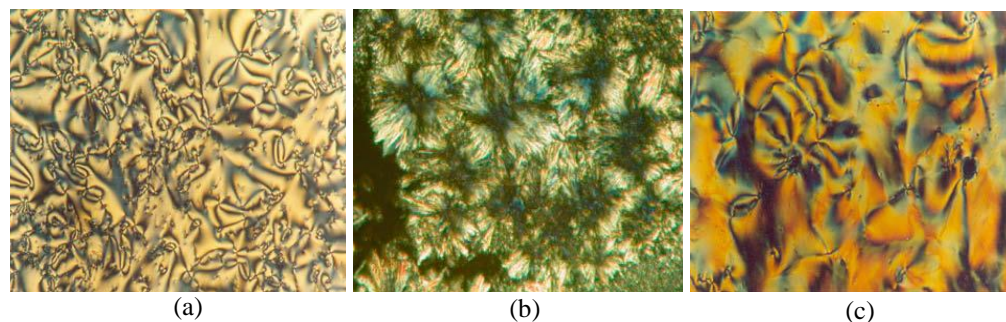


Figure 2.18 Optical textures of: (a) H_2L^1 (SmC), (b) $[\text{La}(\text{L}^1\text{H}_2)_3\text{NO}_3](\text{NO}_3)_2$ (SmX) and (c) $[\text{Pr}(\text{L}^1\text{H}_2)_3\text{NO}_3](\text{NO}_3)_2$ (SmF)

Basova *e al.* [32] reported the mesogenic properties of copper octahexylthiophthalocyanine $[(\text{C}_6\text{S})_8\text{PcCu}]$ (**Figure 2.19(a)**) which shows a columnar hexagonal (Col_h) mesophase (**Figure 2.19(b)**) at room temperature with an extraordinary phase range of more than 300°C . The complex did not form isotropic liquid until 350°C and the mesophases were apparently stable up to about $300\text{--}350^\circ\text{C}$, where the material started to decompose.

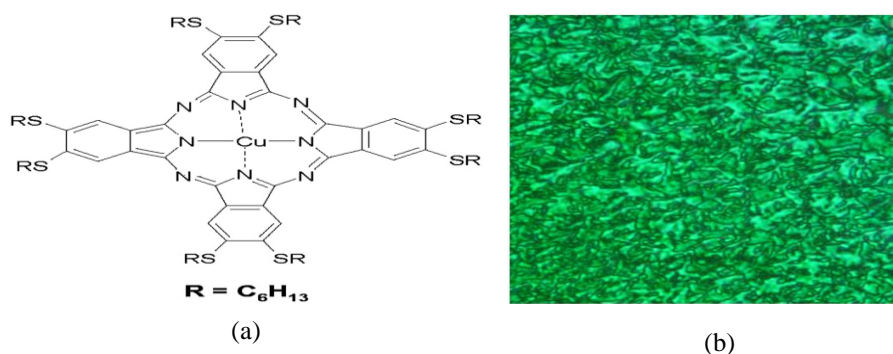


Figure 2.19 $[(\text{C}_6\text{S})_8\text{PcCu}]$ (a) structural formula; (b) columnar hexagonal (Col_h) mesophase

2.2.3 Magnetism

The study of magnetic properties of materials is called magnetochemistry. The understanding of magnetism is closely related to the concept of spin which arises from the relativistic description of an electron in an external electromagnetic field. This concept results in the spin magnetic moment and the orbital magnetic moment, which is due to the motion of electronic charges.

Magnetic materials can be classified into three classes: diamagnetism, paramagnetism and cooperative magnetism [47]. In diamagnetic materials, the electron spins are paired and aligned parallel to the applied magnetic field. Diamagnetism is a property of all materials. Some examples of diamagnetic materials are nearly all organic compounds, metals such as Hg, and superconductors below the critical temperature (temperature at a critical state or at which a phase boundary ceases to exist).

Paramagnetic materials have unpaired electrons, and the magnitude of the paramagnetism depends on the number of unpaired electron(s), with spin aligned randomly in the absence of an applied magnetic field (**Figure 2.20**). Many transition metal salts and complexes are paramagnetic because of the partially filled *d*-orbitals. Examples are complexes of Cr^{3+} (three unpaired electrons) and Cu^{2+} (one unpaired electron).

Cooperative magnetism is the result of an exchange interaction between permanent magnetic dipoles. It can be divided into three categories: ferromagnetic, antiferromagnetic and ferrimagnetic.

In a ferromagnetic substance, there are unpaired electron spins, which are held in alignment by a process known as ferromagnetic coupling. Ferromagnetic compounds, such as iron(II) and iron(III), are strongly attracted to magnets.

In an antiferromagnetic compound, the unpaired electron is held in an alignment with an equal number of spins in each direction, resulting in a strong repulsion by a magnet.

In contrast, ferrimagnetic compounds have unpaired electron spins, which are held in a pattern with some up and some down. This is known as ferrimagnetic coupling. In these compounds, there are more spins held in one direction, so the compound is attracted to a magnet [57].

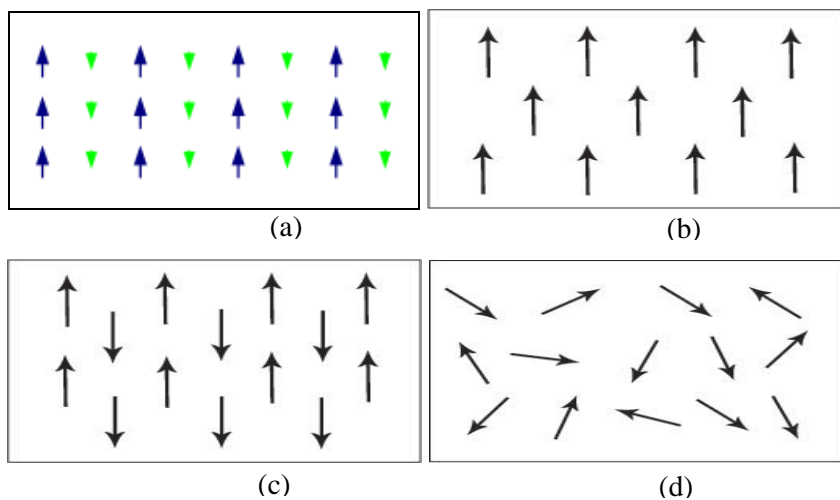


Figure 2.20 *Magnetic ordering: (a) ferrimagnetic materials; (b) ferromagnetic materials; (c) antiferromagnetic materials; and (d) paramagnetic materials*

The magnetic properties of a compound can be deduced from its effective magnetic moment (μ_{eff}), calculated using the following relationship:

$$\mu_{\text{eff}} = 2.828(\chi_{\text{M}}^{\text{corr}}\text{T})^{1/2}$$

where χ_M^{corr} is the corrected molar magnetic susceptibility, and T is the temperature in kelvin (K).

The value of χ_M^{corr} at room temperature can easily be determined using a Gouy balance (**Figure 2.21**). This instrument consists of a sensitive balance from which the sample hangs and lies in between the poles of magnet. The balance may be calibrated against a standard with an accurately known susceptibility, such as H_2O (-0.77×10^{-6} c.g.s), $\text{CoCl}_2 \cdot \text{H}_2\text{O}$ ($+4.081 \times 10^{-5}$ c.g.s), $\text{MnSO}_4 \cdot \text{H}_2\text{O}$ ($+6.52 \times 10^{-5}$ c.g.s), $\text{CuSO}_4 \cdot 5\text{H}_2\text{O}$ ($+0.6 \times 10^{-5}$ c.g.s) or $\text{Hg}[\text{Co}(\text{SCN})_4]$ ($+1.644 \times 10^{-5}$ c.g.s).



Figure 2.21 Gouy balance

The value directly obtained from the Gouy balance is the gram susceptibility, χ_g . The next steps are to calculate the diamagnetic contribution, χ_{dia} , of each atom in the molecule from the Pascal's constant (**Appendix 2**), and then the molar susceptibility, χ_m , by multiplying the value of χ_g with the molecular weight. The value of χ_M^{corr} is then obtained from the relationship: $\chi_M^{\text{corr}} = \chi_m - \chi_{\text{dia}}$.

The effective magnetic moment (μ_{eff}) provides information about the number of unpaired electrons from the spin-only relationship: $\mu_{\text{eff}} = [n(n+2)]^{1/2}$, where n is the number of unpaired electron(s), and hence the distinction between

high spin and low spin in octahedral complexes, spectral behavior, and structure of a complex.

For example, the valence electronic configuration of copper(II) is $3d^9$, and thus has one unpaired electron and should form paramagnetic complexes with the expected μ_{eff} of 1.73 B.M. Most copper(II) complexes reported have magnetic moments in the range of 1.8-2.0 B.M., indicating either a mononuclear complex or a multinuclear complex with no spin coupling between the unpaired electrons of the copper(II) centres. However, there are also complexes with subnormal moments (less than 1.73 B.M.).

Konar et al. reported that polymeric $[\text{Cu}(\text{pyrazine-2,3-dicarboxylate})(\text{H}_2\text{O})_2]\cdot\text{H}_2\text{O}$ (**Figure 2.22**), which has the *syn-anti* carboxylate bridge [34], has J value of -0.5 cm^{-1} , suggesting weak antiferromagnetic interaction. These authors suggested that the almost negligible coupling between the Cu(II) centres in their complex was because of the reduction of the magnetic pathway as the basal ligand was well directed ($d_{x^2-y^2}$ magnetic orbital) but the axial ligand was unfavourably located (d_z^2 orbital).

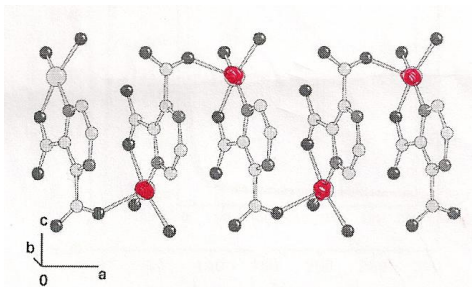


Figure 2.22 The crystal structure of polymeric $[\text{Cu}(\text{pyrazine-2,3-dicarboxylate})(\text{H}_2\text{O})_2]\cdot\text{H}_2\text{O}$

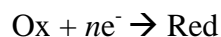
Kandaswamy *et al.* [33] reported that a dark green complex, $[\text{Cu}_2\text{L}(\text{ClO}_4)_2] \cdot 2\text{CH}_3\text{OH} \cdot 2\text{H}_2\text{O}$, where L was from the dianion of (*N,N*-bis{2-hydroxy-5-methyl-3-(morpholin-1-ylmethyl)benzyl}-*N',N'*-diethyl-1,3-propanediamine has magnetic moment at room temperature of 1.51 B.M., which is less than the spin-only value of 1.73 B.M. This indicates the occurrence of an antiferromagnetic exchange interaction within the molecule. The singlet-triplet energy separation ($-2J$), calculated using the Bleaney-Bowers equation (**Equation 2.1**) for dinuclear complexes, was 112 cm^{-1} , suggesting that the complex has a weak antiferromagnetic coupling between the two Cu(II) centers.

$$-2J = \{ \ln[\{ 1.2186 \times 10^{-2} / (\chi_m - 0.12 \times 10^{-3}) \} - 3] \} 207. \quad \text{Equation 2.1}$$

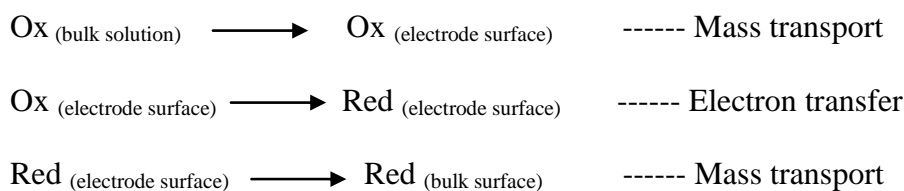
where χ_m is the paramagnetic susceptibility per Cu(II) after the correction for diamagnetism, and $2J$ is the singlet-triplet energy separation.

2.2.4 Redox properties

Electrochemistry is the study of the effect of addition or removal of electron from the molecular frames or in the other hand, to study the relationship between chemical changes and the electron flow [50]. The reaction at the electrode is always heterogeneous. The electrode reaction can be formulated by redox reaction. Redox can be defined as **Reduction** and **Oxidation** of any chemical substances that take place during the chemical reaction.



At first, the electrode must be in touch with the reagent (Ox), then the heterogeneous electron transfer process from the solid electrode to the species Ox must take place and finally, the reduced product (Red) must be removed from the electrode surface in order to allow the access of further amount of Ox to the electrode surface.



There are many conventional techniques that have been used to study electrochemistry. An example is cyclic voltammetry (CV).

CV is a type of potentiodynamic electrochemical measurement [58]. In CV, the electrode potential ramps linearly. This ramping is known as scan rate (V/s). The potential is applied between the reference electrode and the working electrode and the current is measured between the working electrode and the counter electrode. This data is then plotted as current (i) vs. potential (E). The forward scan produces a current peak for any analytes that can be reduced (or oxidized depending on the initial scan direction) through the range of the potential scanned. The current will increase as the potential reaches the reduction potential of the analyte, but then falls off as the concentration of the analyte is depleted close to the electrode surface. If the redox couple is reversible, then when the applied potential is reversed, it will reach the potential that will reoxidize the

product formed in the first reduction reaction, and produce a current of reverse polarity from the forward scan. This oxidation peak will usually have a similar shape to the reduction peak. As a result, information about the redox potential and electrochemical reaction rates of the compounds is obtained.

Voltammetric techniques involve the electrolysis of the solution to be analyzed using a controlled external power source and measuring the resultant current potential or current time curves to obtain information about the solution. The species to be determined undergoes oxidation or reduction at a working electrode. The voltage between the working electrode and an auxiliary or counter electrode is controlled by the external circuitry in order to maintain a preselected potential difference at the working electrode, with respect to the reference electrode, as a function of time [56].

In CV, three electrodes are immersed in a solution containing the analyte and an excess of electrolyte, such as tetrabutylammonium tetrafluoroborate [36], tetraethylammonium perchlorate [10], or tetrabutylammonium perchlorate [6]. One of the three electrodes is the working electrode, which is typically made of platinum, gold, silver, glassy carbon, nickel, or palladium. The second electrode is the reference electrode, which provides calibration for the applied potential. The third electrode is the counter electrode, which is often a platinum wire that simply serves to conduct electricity from the signal source through the solution to the other electrodes [60].

CV is a very useful technique since it provides a fast and simple method for initial characterization of a redox-active system, information about the rate of

electron transfer between the electrode and the analyte and the stability of the analyte in the electrolyzed oxidation states.

It is noteworthy that in CV, there are some types of reactions such as reversible reaction, irreversible reaction and quasi-reversible reaction. The characteristics for reversible reaction are the voltage separation between the current peaks is 59 mV, the positions of peak voltage do not alter as a function of scan rate, the ratio of the peak current is equal to one and the peak currents are proportional to the square root of the scan rate [59].

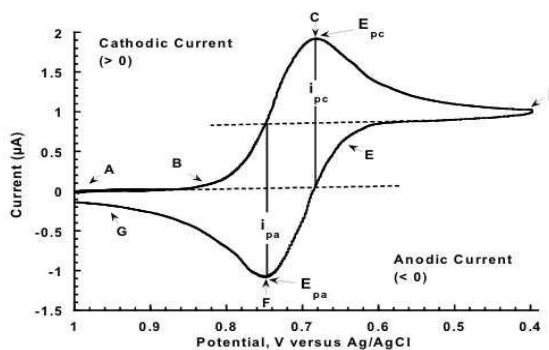


Figure 2.23 An example of a cyclic voltammogram

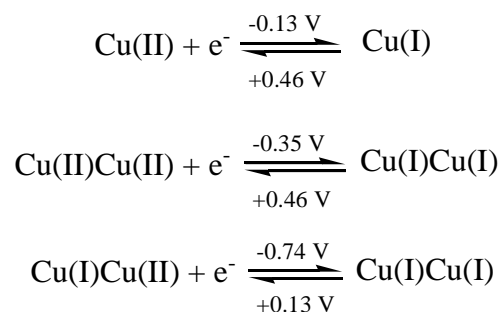
In irreversible processes [50], the potential at which the reduction ($\text{Ox} + n\text{e}^- \rightarrow \text{Red}$) takes place can be much more cathodic than the formal electrode potential of the couple Ox/Red. In addition, the separation between the forward peak (p_f) and the reverse peak (p_r) is large, so that the reversed peak is undetected. The characteristics of the irreversible process are the forward peak potential shifts with the scan rate, ν (towards more cathodic values for reduction processes), the current function $i_{pf}/\nu^{1/2}$ is constant and no current ratio i_{pr}/i_{pf} exists.

The quasi-reversible processes occur in the transition zone between the reversible and irreversible processes [50]. It occurs when the rate of electron transfer is of the same magnitude as the mass transport. The characteristics of quasi-reversible processes are the forward peak potential, E_{pf} shifts (towards more negative potential values for reduction steps) with scan rate (ΔE_p value at 25°C is higher than $59/n$ (mV), the current of the forward peak (i_{pf}) increases with $v^{1/2}$, and the current ratio i_{pr}/i_{pf} is equal to 1 only if the transfer coefficient, $\alpha = 0.5$. The value of $i_{pr}/i_{pf} < 1$ for $\alpha > 0.5$, and $i_{pr}/i_{pf} > 1$ for $\alpha < 0.5$.

For example, Kandaswamy *et al.* [35] determined the electrochemical behavior of $[\text{Cu}_2\text{L}^1(\text{OAc})](\text{ClO}_4)_2 \cdot 2\text{H}_2\text{O}$ where $\text{L}^1 = 2,6\text{-bis}\{N\text{-}[2\text{-(2-benzimidazolyl)}]\text{-4-methylphenol}$ in DMF. The electrochemical data revealed that the complex undergo reduction at highly negative potential ($E_{pc}^1 = -0.45$ V, $E_{pc}^2 = -1.10$ V). This is due to the factors such as restricted free rotation of the imino linkage and planarity induced by complete conjugation; a rigid ligand network and direct attachment of the benzimidazole ring to the phenyl residue of the ligand will stabilize the Cu(II) oxidation state making the Cu(II) to Cu(I) conversion more difficult.

Isa *et al.* [36] reported the CV for copper(II) benzoate, $[\text{Cu}_2(\text{C}_6\text{H}_4\text{COO})_4] \cdot (\text{C}_2\text{H}_5\text{OH})_2$ in methanolic:ethanoic acid solution (20:1 v/v) measured from +1.5 V to -1.0 V with the scan rate of 150 mV/s. The complex showed three reduction peaks at -0.13, -0.35 and -0.74 V, and two overlapping anodic peaks at +0.31 V and +0.46 V. The presence of three reduction peaks reveals the existence of multiple species in the solution possibly due to partial

dissociation of the complex to mononuclear units. The peak current for this complex varies with the scan rate ranging from 400 mV to 1200 mV, indicating that the complex undergoes extensive structural reorganization upon reduction. In addition, the ratio of I_{pc}/I_{pa} is less than unity, suggesting that the complex experienced electron transfer followed by a chemical reaction. The possible redox reactions mechanism for the complex is:



Koo [10] reported the CV for mononuclear $[\text{Cu}(\text{CH}_3\text{COO})_2(\text{bpy})]$ in DMSO solution in the range +0.5 to -2.10 V. The complex show the existence of two cathodic processes at E_p values of -0.54 and -1.66 V and a broad peak on the reverse scan assignable to oxidation of copper metal deposited on the electrode surface. The reversal of the potential scan at -1.40 V exhibited that the first process to be quasi-reversible: $E_{1/2} = -0.37 \text{ V}$ ($\Delta E_p = 0.35 \text{ V}$, $I_{pc}/I_{pa} = 1.38$). The CV process of the complex is:



2.3 INSTRUMENTAL TECHNIQUES FOR STRUCTURAL ELUCIDATION

2.3.1 *Elemental Analyses*

Elemental analyzer (**Figure 2.24**) is an essential instrument in analyzing the composition of an unknown sample(s). The analysis can be qualitative (determining what elements are present) or quantitative (determining the percentage of the element present), and the sample may be a solid or a liquid.

In this technique, a sample (about 1-3 mg) is burned in an excess of oxygen, and various traps collect the combustion products, carbon dioxide, water, and nitric oxide. The weights of these combustion products can be used to calculate the composition of carbon, hydrogen and nitrogen respectively, in the unknown sample.

There are different techniques for the determination of CHN \ CHNS \ O. It brings a new level of precision, accuracy, speed of analysis and ease of operation. The built-in chromatographic column converts the compound and elutes it in the form of NO₂, CO₂, SO₂, H₂O which are then detected with the help of a thermal conductivity detector (TCD). The key components of CHNS are auto sampler, combustion reactors, chromatographic column, and TCD. The most common form of elemental analysis, the CHN analysis, is accomplished by combustion [61].

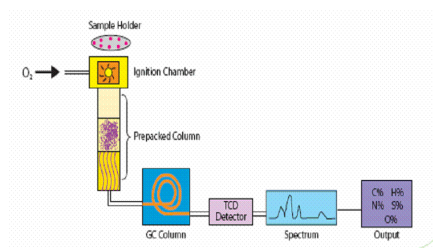


Figure 2.24 A schematic diagram of a *CHN analyzer*

The instrument is calibrated with the analysis of standard compounds using the K-factors calculations. Thus the instrument ensures maximum reliability of the results because the combustion gases are not split or diluted but directly carried to built-in GC system. Simultaneous determination of CHNS can be done in less than 10 mins. This method finds greatest utility in finding the percentages of C, H, N, S, (O) in organic compounds which are generally combustible at 1800°C.

2.3.2 Fourier Transform Infrared Spectroscopy

Infrared spectroscopy is the study of interaction of infrared light with matter based on the vibration of the atoms of a molecule [51]. The most common type of spectrometer nowadays is called Fourier Transform Infrared (FTIR). The spectrum may be recorded for organic and inorganic samples, if they can absorb light energy with the frequency in the IR region at 4000-400 cm^{-1} [52].

A molecule should have a change in its dipole moment during the vibration in order to be IR active. For example, the heteronuclear diatomic molecule such as CO_2 molecule which undergoes asymmetric stretching is IR active whereas if CO_2 molecule undergoes the symmetric stretching, the molecule now is IR inactive.

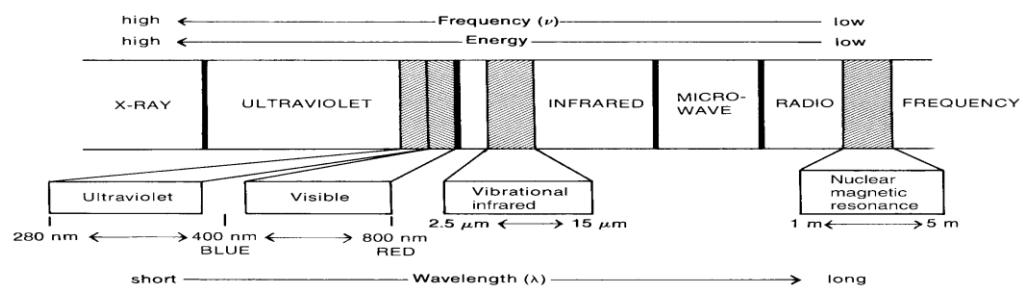


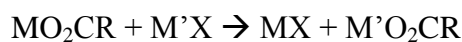
Figure 2.25 *The region of electromagnetic spectra*

The determination of FTIR can be done with solids, liquids or gases samples. For solid, there are three common techniques to record the solid spectra, either by using KBr disk, mulls or deposited film. Solid sample normally were mixed with KBr and were ground with agate mortar and pestle [51]. For liquid samples, a drop of the sample is placed on the salt plate, such as sodium chloride or potassium chloride. In this technique, the plates are squeezed to form a thin liquid film. The sample must be free from water since the salt plate is water soluble [53]. Gas samples at pressures up to 1 atm or greater are usually contained in glass cell either 5 or 10 cm long closed at the end with rock salt windows [52].

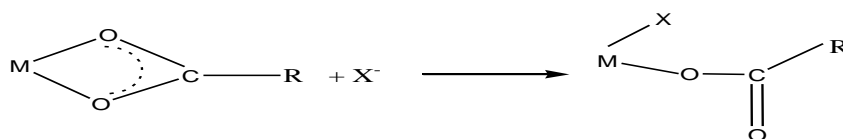
FTIR spectroscopy might work well on certain samples and might not be helpful to analyze some samples. Some of the advantages of FTIR are: (a) can be used to analyze solid, liquid, gases as well as polymer samples; (b) the peaks positions, intensities, widths, and shape in the spectrum give useful information; and (c) the analysis, including sample preparation, and scanning can be done in a short time.

However, not all samples are IR active. A molecule must have a chemical bond in order to absorb the IR radiation and to give the FTIR spectrum. A monoatomic ions, such as Pb^{2+} in water, does not absorb IR radiation and thus do

not have IR spectra. FTIR also cannot detect homonuclear diatomic molecules such as O=O, and N≡N due to their symmetry aspect. In complex molecules, the FTIR spectrum can be very complicated with overlapping peaks, making individual peak assignment impossible or very difficult. Furthermore, Deacon et al. [37] reported that examination of carboxylates complex in solution or as mulls between alkali halide plates or in potassium halide discs can result in anion exchange.



In addition, formation of potassium halide discs may result in pressure induced changes of spectra. For example, $\nu_{\text{asym}}(\text{CO}_2)$ of potassium formate is at 1581 cm^{-1} in Nujol but shift to 1630 cm^{-1} in a KBr disc. Obviously, pressure can enhance anion exchange between the complex and the disc materials. Furthermore, pressure could promote hydrolysis of $\text{M}(\text{O}_2\text{CR})$ groups by coordinated water or by trace moisture in the disc material. In addition, pressure induced coordination of halide ions could change the nature of carboxylate coordination.



There are several ways that a carboxylate ligand (RCOO^-) may coordinate to a metal ion (**Figure 2.26**).

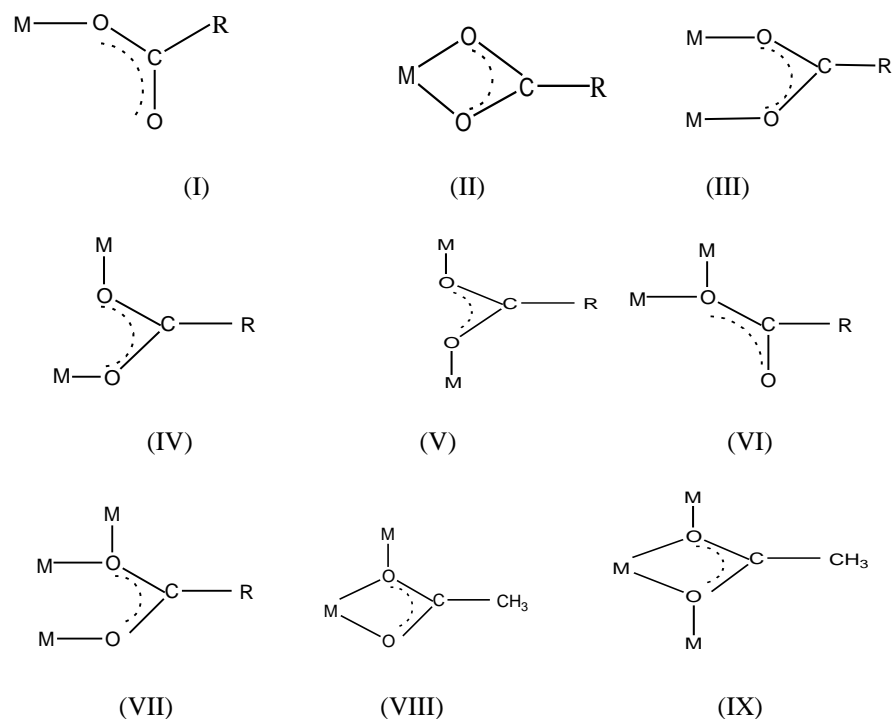


Figure 2.27 Different binding modes of carboxylate group: (I) unidentate; (II) chelating; (III) bridging bidentate in syn-syn configuration; (IV) bridging bidentate in syn-anti configuration; (IV) bridging bidentate in anti-anti configuration; (V) monoatomic bridging; (VI) monoatomic bridging additional bridging; (VIII) and (IX) both chelating and bridging

In addition, Deacon *et al.* [37] also reported that the different coordination modes of the carboxylate ligands can be deduced using FTIR, from the difference in the values of asymmetric (ν_{asym}) and symmetric (ν_{sym}) stretching COO vibrations ($\Delta = \nu_{\text{asym}} - \nu_{\text{sym}}$). The ν_{asym} and ν_{sym} values are normally observed as strong peaks at about 1600 cm^{-1} and 1400 cm^{-1} , respectively. The value of Δ for unidentate RCOO is larger than 200 cm^{-1} , ionic RCOO is 164 cm^{-1} , and bridging or chelating RCOO is less than 164 cm^{-1} (normally the Δ value for chelating is less than Δ value for bridging).

For example, Rosu *et al.* [38] reported Cu(II) complex with 1-phenyl-2,3-dimethyl-4-(N-3-formyl-6-methyl-chromone)-3-pyrazolin-5-one (HL) (**Figure**

2.28) by adding a hot methanolic solution of HL to $\text{Cu}(\text{OAc})_2 \cdot \text{H}_2\text{O}$ in aqueous/methanolic solution (1:2 v/v). The IR of the complex reveal that $\nu(\text{C}=\text{O})$: 1634 cm^{-1} ; $\nu(\text{C}=\text{N})$: 1608 cm^{-1} ; $\nu(\text{Ar}-\text{OH})$: 1125 cm^{-1} ; $\nu(\text{Ar}-\text{O}_{\text{aliphatic}})$ 1243 cm^{-1} ; $\nu_{\text{asym}}(\text{CH}_3\text{COO}^-)$: 1683 cm^{-1} ; $\nu_{\text{sym}}(\text{CH}_3\text{COO}^-)$: 1393 cm^{-1} and Δ of the complex is 290 cm^{-1} which is monodentate nature of coordinated acetate group.

Sletten *et al.* [39] reported the binuclear Cu(II) complex of formula, $[\text{Cu}_2(\text{bpca})_2(\text{H}_2\text{O})_3(\text{SO}_4)] \cdot \text{H}_2\text{O}$ where bpca = bis(2-pyridylcarbonyl)amide anion by adding a dissolved sodium sulfate in a hot water to a warm solution of $[\text{Cu}(\text{bpca})(\text{H}_2\text{O})_2]\text{NO}_3$ to yield a sky blue rod crystal. The IR of the complex showed $\nu(\text{H}_2\text{O})$: 3430 cm^{-1} ; $\nu_{\text{asym}}(\text{CO}$ of amide): 1710 cm^{-1} ; $\nu_{\text{asym}}(\text{COO}$ of oxalate ligand): 1640 cm^{-1} ; $\nu_{\text{sym}}(\text{COO}$ of oxalate ligand): 1350 cm^{-1} ; $\nu(\text{coordinated sulphate})$: $620, 1115$ and 1150 cm^{-1} . The value of Δ of the complex is 290 cm^{-1} , indicating a monodentate binding mode of the carboxylate ligand.

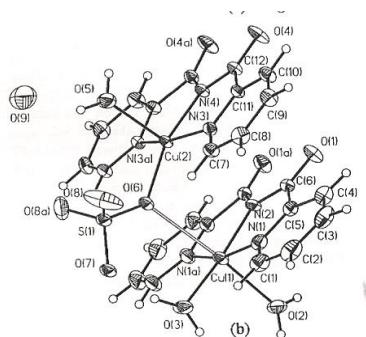


Figure 2.29 The crystal structure of $[\text{Cu}_2(\text{bpca})_2(\text{H}_2\text{O})_3(\text{SO}_4)] \cdot \text{H}_2\text{O}$

2.3.3 UV-visible Spectroscopy

The UV-vis spectroscopy deals with electronic transitions, from lower to higher energy levels. The excitations of electron(s) can occur between a bonding or lone

pair orbital and an unoccupied non-bonding or antibonding orbital. The electronic energy levels and electronic transitions are shown in **Figure 2.30**.

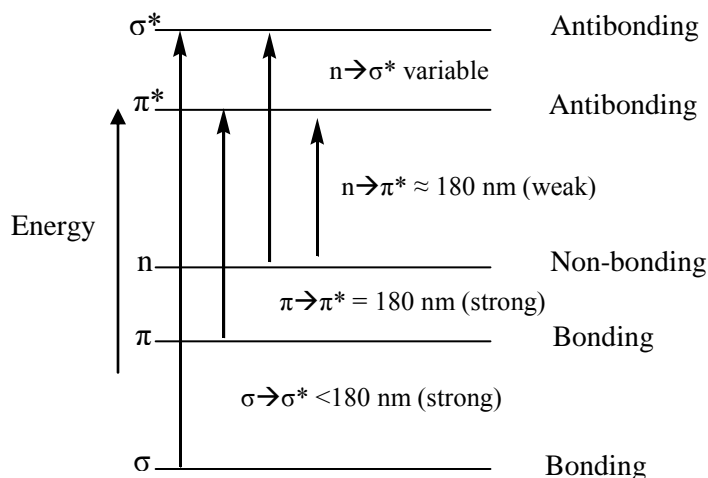


Figure 2.30 *Electronic energy levels and electronic transitions*

Most UV-vis spectrometers consist of light source normally built up from a tungsten-filament lamp (scanning visible region) and hydrogen or deuterium discharge tube (scanning near UV region), sample and reference cells which were made from silica or quartz, a wavelength selection device or monochromator to spread out the wavelength either by using prisms or diffraction grating and a detector to receive the radiation and then transfer into spectrum

Copper(II) ion in carboxylate complexes has one unpaired $3d$ electron. Thus, their UV-vis spectrum normally shows a broad $d-d$ band in the region of 600 nm to 800 nm, assigned to the $d-d$ electronic transition. The position of the band may be used to deduce the geometry at Cu(II) centre, while the molar absorptivity is an indicator for the nuclearity of a complex. It is also noted that the ϵ values for most mononuclear Cu(II) complexes are about $100 \text{ M}^{-1} \text{ cm}^{-1}$ [10,

40-41], while the value is about $600 \text{ M}^{-1} \text{ cm}^{-1}$ for a tetranuclear Cu(II) complex [42].

Wang *et al.* [43] reported the mixed-valence Cu(I,II) α,β -unsaturated carboxylate complexes with triphenylphosphine and methanol ligand, $[\text{Cu}_2^{\text{I}}\text{Cu}_2^{\text{II}}\text{A}_6(\text{PPh}_3)_4(\text{CH}_3\text{OH})_2]$ (A is $\text{CH}_2=\text{CHCOO}^-$). The complex was synthesized by adding a methanolic solution of PPh_3 to a methanolic solution of $[\text{Cu}_2(\text{CH}_2=\text{CHCOO})_4]$ to yield a pale-green crystals after several days. From electronic reflectance spectroscopy recorded from 200-1100 nm, the complex shows a square pyramidal geometry around Cu(II) centers. The intense reflectance band at higher frequency assigned as the intraligand transitions (210-264 nm), the carboxylate-to-copper charge transfer band (LMCT) was observed at 380 nm and the visible reflectance band at 740 nm with a shoulder at 1024 nm are characteristic of Cu(II) $d_{xz}, d_{yz} \rightarrow d_{x^2-y^2}$ (${}^2\text{E} \rightarrow {}^2\text{B}_1$) transitions in tetragonal field. The shoulder is a characteristic of a bridging system with antiferromagnetic interaction.

Narayanan *et al.* [44] reported the mononuclear Cu(II) of 2,6-bis(4-methylpiperazin-1-yl-methyl)-4-acetylphenol (HL^1), $[\text{CuL}^1(\text{CH}_3\text{COO})]\cdot\text{H}_2\text{O}$ by adding a methanolic solution of the ligand HL^1 to a methanolic solution of $\text{Cu}(\text{CH}_3\text{COO})_2\cdot\text{H}_2\text{O}$ under 4 hours reflux to yield a dark green compound that was further recrystallized from acetonitrile. The electronic spectrum of the complex in methanol reveals from the $d-d$ transition at 597 nm ($\epsilon_{\text{max}}/\text{M}^{-1}\text{cm}^{-1}$, 132) suggesting square planar geometry, at 358 nm ($\epsilon_2/\text{M}^{-1}\text{cm}^{-1}$, 17900) suggesting the phenolate-to-copper charge transfer, and at 294 ($\epsilon_3/\text{M}^{-1}\text{cm}^{-1}$, 24100) indicating intraligand charge-transfer transition.

2.3.4 Molar Conductance

Molar conductance is a measure of ionic motion in solution. The number of ions in a solution is normally expressed by the molar conductivity, Λ_m , which can be calculated using the following equation:

$$\Lambda_m = 1000\kappa/c$$

where, κ is the conductivity ($S\text{ cm}^{-1}$) and c is molar concentration (M). The SI unit for Λ_m is $S\text{ cm}^2\text{ mol}^{-1}$.

Geary [45] reported that the selection of electrolyte or solvent for conductivity determination depends on its dielectric constant, viscosity, specific conductivity, ease of purification and donor capacity towards metal ions. **Table 2.2** shows the expected Λ_m range for different type of electrolytes.

Table 2.2 The expected Λ_m for complexes of different electrolyte types at 10^{-3} M in the common organic solvent ($S\text{ cm}^2\text{ mol}^{-1}$)

Solvent	Electrolyte			
	1:1	2:1	3:1	4:1
Nitromethane	75-95	150-180	220-260	290-330
Nitrobenzene	20-30	50-60	70-82	90-100
Acetone	100-140	160-200	270	360
Acetonitrile	120-160	220-300	340-420	500
Dimethylformamide	65-90	130-170	200-400	300
Methanol	80-115	160-220	290-350	450
Ethanol	35-45	70-90	120	160

REFERENCES

- [1] G. S. Attard and P. R. Cullum, *Liquid Crystals*, **8(3)** (1990) 299 – 309.
- [2] W. E. Hatfield, C. S. Fountain, and R. Whyman, *Inorg. Chem.*, **5(11)** (1966) 1855-1858.
- [3] F. Cariati, L. Erre, G. Micera, A. Panzanelli, G. Ciani, and A. Sironi, *Inorganica Chimica Acta*, **80** (1983) 57-65.
- [4] L. Strinna Erre, G. Micera, P. Piu, F. Cariati, and G. Ciani, *Inorg. Chem.* **24** (1985) 2291-2300.
- [5] L. S. Erre and G. Micera, *Polyhedron* Vol. 6, No. 10, pp 1869-1874, 1987.
- [6] S.P. Perlepes, E.Libby, W. E. Streib, K. Folting and G. Christou, *Polyhedron*, **11(8)** (1992) 923-936.
- [7] W. Zhang, S. Liu, C. Ma and D. Jiang, *Polyhedron*,**17(22)** (1998) 3835 – 3839.
- [8] P.Kogeler, P.A.M.Williams, B.S.Parajon-Costa, E.J.Baran, L.Lezama, T.Rojo, A.Muller, *Inorganica Chimica Acta*, **268** (1998) 239-248.
- [9] N. Abdullah, Z.A. Kamarazaman. *AIP Conf. Proc.*, 1136 (2009) 361.
- [10] B.K.Koo, *Bull.Korean Chem.Soc.*, **22(1)** (2001) 113-116.
- [11] H.Nunez, J.S.Carrio, E.Escrivia, L.Soto, J.G.Lozano, A.Sancho, B.Verdejo, E.G.Espana, *Polyhedron*, **27** (2008) 633-640.
- [12] C.Yenikaya, M.Poyraz, M.Sari, F.Demirci, H.Ilkimen, O.Buyukgungor, *Polyhedron*, **28** (2009) 3526-3532.
- [13] M.Melnik, M.D.Jurco, *Inorganica Chimica Acta*, **86** (1984) 185-190.
- [14] S.Youngme, A.Cheansirisomboon, C.Danviturai, C.Pakawatchai, N.Chaichit, C.Engkagul, G.A.van Albada, J.S.Costa, J.Reedijk, *Polyhedron*, **27(7)**, (2008) 1875-1882.
- [15] H.Hadadzadeh, S.J.A.Fatemi, S.R.Hosseinian, H.R.Khavasi, R.Pottgen, *Polyhedron*, **27(1)** (2008) 249-254.
- [16] M.Inoue, M.Kishita, M.Kubo, *Inorg.Chem.*, **3(2)** (1964) 239.
- [17] A.M.Donia, *Thermochimica Acta*, **320** (1998) 187-199.
- [18] G.Micera, P.Piu, L.S.Erre, *Thermochimica Acta*, **84** (1985) 175-182.
- [19] W.Brzyska, W.Wolodkiewicz, *Thermochimica Acta*, **242** (1994) 131-140.

- [20] A.M. Giroud-Godquin. *Coord. Chem. Rev.*, **178** (1998) 1485.
- [21] R. Giménez, D.P. Lydon, J.L. Serrano. *Curr. Opin. Solid State Mater. Sci.*, **6** (2002) 527.
- [22] R.W. Date, E.F. Iglesias, K.E. Rowe, J.M. Elliott, D.W. Bruce. *Dalton Trans.*, (2003) 1914.
- [23] A. Crispini, M. Ghedini, D. Pucci. *Beilstein J. Org. Chem.*, **5(54)** (2009) 1.
- [24] R.W.Date, E.F.Iglesias, K.E.Rowe, J.M.Elliot, D.W.Bruce, *Dalton Trans.* (2003) 1914-1931. DOI: 10.1039/b212610a.
- [25] G.Godquin, A.M., Marchon, J.C., Guillon, D., Skoulios, A., *J. Phys. Lett.*, Paris, **45** (1984) L681.
- [26] Abied, H., Guillon, D., Skoulios, A., Weber, P., G.Godquin, A.M., Marchon, J.C., *Liq Crystals*, **2** (1987) 269.
- [27] G.Godquin, A.M., Marchon, J.C., Maldivi, P., Aldebert, P., Peguy, A., Skoulios, A., *J. Phys.*, Paris, **50** (1989) 513.
- [28] Abied, H., Guillon, D., Skoulios, A., Dexpert, H., G.Godquin, A.M., Marchon, J.C., *J. Phys.*, Paris, **49** (1988) 345.
- [29] A.M. G.Godquin, *Coordination Chemistry Review*, **178-180** (1998) 1485-1499.
- [30] A.K.Singh, A.Kumari, T.N.G.Row. J.Prakash, K.R.Kumar, B.Sridhar, T.R.Rao, *Polyhedron*, **27** (2008) 3710-3716.
- [31] S.Kumari, A.K.Singh, K.R.Kumar, B.Sridhar, T.R.Rao, *Inorganica Chimica Acta*, **362** (2009) 4205-4211.
- [32] T.Basova, E.Kol'tsov, A.G.Gurek, D.Atilla, V.Ahsen, A.K.Hassan, *Materials Science and Engineering C*, **28** (2008) 303-308.
- [33] P.Kamatchi, S.Selvaraj, M.Kandaswamy, *Polyhedron*, **24** (2005) 900-908.
- [34] S. Konar, S. C. Manna, E. Zangrando, N. R. Chaudhuri, *Inorganica Chimica Acta*, doi:10.1016/j.ica.2003.12.003.
- [35] P.Amudha, P.Akilan, M.Kandaswamy, *Polyhedron*, Vol. 18 (1998) 1355-1362.
- [36] M. I. Mohamadin, N. Abdullah. *Central European Journal of Chemistry*, **8** 1090 (2010).

- [37] G.B.Deacon, R.J.Philips, *Coordination Chemistry Reviews*, **33** (1980) 227-250.
- [38] T.Rosu, E.Pahontu, C.Maxim, R.Georgescu, N.Stanica, G.L.Almajan, A.Gulea, *Polyhedron*, **29** (2010) 757-766.
- [39] M.L.Calatayud, I.Castro, J.Sletten, F.Lloret, M.Julve, *Inorganica Chimica Acta*, **300-302** (2000) 846-854.
- [40] A. Garcis-Raso, J.J. Fiol, F. Badenas, E. Lago, E. Molins. *Polyhedron*, **20** (2001) 2877.
- [41] X. Liu, E.J.L. McInnes, C.A. Kilner, M. Thornton-Pett, M.A. Halcrow. *Polyhedron*, **20** (2001) 2889.
- [42] E. Kavlakoglu, A. Elmali, Y. Elerman, I. Svoboda. *Polyhedron*, **21**, (2002) 1539.
- [43] Y.Y.Wang, Q.Shi, Q.Z.Shi, Y.C.Gao, X.Hou, *Polyhedron*,**19** (2000) 891-989.
- [44] K.S.Bharati, S.Sreedaran, A.K.Rahiman, K.Rajesh, V.Narayanan, *Polyhedron*, **26** (2007) 3993-4002.
- [45] W.J.Geary, *Coordination Chemistry Review*, **7** (1971) 81-122.
- [46] M.S.Celej, S.A.Dassie, M.Gonzalez, M.L.Bianconi, G.D.Fidelio, *Analytical Biochemistry*, **350** (2006) 277-284.
- [47] M.Getzlaff, *Fundamentals of Magnetism*, Springer, Berlin, 2008.
- [48] P.Atkins, J.D.Paula, *Physical Chemistry*, 7th Ed., Oxford University Press, U.K, 2002.
- [49] O.Kahn, *Molecular Magnetism*, VCH Publishers, U.S.A, 1993.
- [50] P.Zanello, *Inorganic Electrochemistry: Theory, Practice and Application*, Royal Society of Chemistry, U.K, 2003.
- [51] B.Stuart, *Infrared Spectroscopy: Fundamentals and Applications*, John-Wiley and Son, 2004.
- [52] C.N.Banwell, E.M.McCash, *Fundamentals of Molecular Spectroscopy*, 4th Ed., Tata McGraw Hill, U.K, 2004.
- [53] D.L.Pavia, G.M.Lampman, G.S.Kriz, J.R.Vyvyan, *Introduction to Spectroscopy*, 4th Ed., Brooks/Cole Cengage Learning, U.S.A, 2008.

- [54] J.W.Robinson, E.M.S.Frame, G.M.Frame II, *Undergraduate Instrumental Analysis*, 6th Ed, Marcel Dekker, New York, 2005.
- [55] P.Gabbort, *Principles and applications of thermal analysis*, Blackwell Publishing, U.K, 2008.
- [56] F.W.Fifield, D.Kealey, *Principle and Practice of Analytical Chemistry*, 5th Ed., Blackwell Science Ltd., U.K, 2000.
- [57] <http://www.ccl.net/cca/documents/dyoung/topics-orig/magnet.html>
- [58] http://en.wikipedia.org/wiki/Cyclic_voltammetry
- [59] http://www.mpip-mainz.mpg.de/~andrienk/journal_club/cyclic_voltammetry.pdf
- [60] <http://www.csun.edu/~jeloranta/CHEM355L/experiment3.pdf>
- [61] <http://www.rsic.iitb.ac.in/Chn.html> (April 2011)